Self-avoiding walks and polygons on quasiperiodic tilings

2003 J. Phys. A: Math. Gen. 36 6661

(http://iopscience.iop.org/0305-4470/36/24/305)

INSTITUTE OF PHYSICS PUBLISHING JOURNAL OF PHYSICS A: MATHEMATICAL AND GENERAL

J. Phys. A: Math. Gen. **36** (2003) 6661–6673 PII: S0305-4470(03)59117-X

Self-avoiding walks and polygons on quasiperiodic tilings

A N Rogers[1], **C Richard**[2] **and A J Guttmann**[1]

[1] Department of Mathematics and Statistics, University of Melbourne, Victoria 3010, Australia
[2] Institut für Mathematik, Universität Greifswald, Jahnstr. 15a, 17487 Greifswald, Germany

Received 3 February 2003, in final form 18 March 2003
Published 5 June 2003
Online at stacks.iop.org/JPhysA/36/6661

Abstract

We enumerate self-avoiding walks and polygons, counted by perimeter, on the quasiperiodic rhombic Penrose and Ammann-Beenker tilings, thereby considerably extending previous results. In contrast to similar problems on regular lattices, these numbers depend on the chosen initial vertex. We compare different ways of counting and demonstrate that suitable averaging improves convergence to the asymptotic regime. This leads to improved estimates for critical points and exponents, which support the conjecture that self-avoiding walks on quasiperiodic tilings belong to the same universality class as self-avoiding walks on the square lattice. For polygons, the obtained enumeration data do not allow us to draw decisive conclusions about the exponent.

PACS numbers: 02.70.−c, 05.50.+q, 61.44.Br

1. Introduction

Quasiperiodic tilings are most widely used for the description of quasicrystals. With appropriate atomic decorations of the vertices, they serve as structure models which explain physical properties of quasicrystals [10]. From a theoretical point of view, they are idealizations of real substances on which the usual models of statistical physics such as the Ising model may be studied [25, 28, 29]. Quasiperiodic tilings arose before the discovery of quasicrystals, however, more as an object of aesthetic interest in geometry [20, 27].

From a combinatorial point of view, they provide an interesting example of a non-periodic yet structured graph where typical problems of combinatorics such as the counting of objects on a lattice become more complex. This is fundamentally different from counting problems on semiregular lattices, where the underlying translational invariance is still present [17], and also from self-similar graphs, where the self-similarity allows for the solvability of some counting problems.

Consider for example the counting problem of n-step walks on a quasiperiodic tiling. This number depends on the chosen starting point. On a lattice, this phenomenon does not occur

due to translation invariance. Questions arise, such as whether the universal properties of the walks such as critical exponents [26] are changed for quasiperiodic tilings[3], and how different ways of counting affect asymptotic properties. The first question has been investigated for self-avoiding walks (SAWs) and self-avoiding polygons (SAPs). These are walks or loops which do not visit the same vertex twice. Extrapolation of exact enumeration data for a number of quasiperiodic tilings [5, 28] indicates that the critical exponents γ for SAWs and α for SAPs are consistent with the corresponding values on regular lattices $\alpha = 1/2$ and $\gamma = 43/32$. In [22], the related problem of SAWs on Penrose random tilings [15] has been studied by Monte Carlo simulations, the results suggesting the same mean square displacement exponent as in the lattice situation. The studies [5, 28] suffered however from strong finite-size effects due to the relatively short series data available. This is mainly due to the fact that the finite-lattice method [9], being the most successful method known to date for walk enumeration on regular lattices [7, 8], cannot easily be applied here, and so we used the slower method of direct counting. The problem in applying the FLM is discussed in section 3, see also [29]. Another reason for the pronounced finite-size behaviour is that the number of walks or loops depends on the chosen starting point. One might suspect that suitable averaging over different starting points reduces these effects, leading to behaviour comparable to the square lattice case. In this paper, we analyse three different methods of counting in detail. Whereas the first one depends on a chosen vertex of the tiling, the last two are averages over the whole tiling.

- *Fixed origin walks.* We count the number of n-step self-avoiding walks emanating from a given vertex. This number depends on the chosen vertex.
- *Mean number of walks.* We count all translationally inequivalent n-step self-avoiding walks which may occur anywhere in the infinite tiling, weighted by their occurrence probability. For tilings with quasicrystallographic k-fold symmetries, these probabilities are numbers in the underlying module $\mathbb{Z}[e^{2\pi i/k}]$. This leads to a generating function which has non-integer coefficients.
- *Total number of walks.* Here we count the number of translationally inequivalent n-step self-avoiding walks which may occur anywhere in the tiling. This number is bigger than the number of fixed origin walks, and by definition, takes into account vertices over the whole tiling.

Note that two self-avoiding walks (polygons) are translationally equivalent iff they have, up to a translation, the same vertex coordinates. For self-avoiding polygons, we will employ the second and the third method of counting. We do not distinguish between different fillings of the interior of the polygon. For SAPs, the second method has been implemented previously [28] to obtain the high temperature expansion of the Ising model. The mean number of SAPs up to length $2n = 18$ has been determined on the Ammann-Beenker tiling [1, 18] and on the rhombic Penrose tiling [6, 27].

We counted SAWs and SAPs on the Ammann-Beenker tiling and the rhombic Penrose tiling and compared different counting schemes, thereby extending and generalizing the previous approaches to counting SAWs [5] and SAPs [28]. Generally speaking, averaging reduces oscillation of data due to finite-size effects, providing improved estimates for critical points and critical exponents. Within numerical accuracy, we cannot rule out the universality hypothesis that SAWs on the Ammann-Beenker and on the rhombic Penrose tilings have the same exponents as on the square lattice. The data for the total number of walks (polygons) give a different exponent, reflecting the fact that the number of patches increases quadratically

[3] For ferromagnetic spin systems on quasiperiodic graphs, a heuristic criterion determines whether its behaviour is different from the lattice situation [25].

with the patch size, in contrast to the lattice case [21, 24]. The limited quantity of SAP data does not allow us to draw decisive conclusions about exponents.

This paper is organized as follows. Sections 2 and 3 describe the algorithms used for the generation of the tilings and for the computation of the numbers of walks and their mean values. Section 4 is devoted to the asymptotic analysis of the series and to a comparison of the different approaches. We concluded with a discussion of possible future work.

2. Graph generation

Quasiperiodic tilings in $\mathbb{R}^d$ may be obtained by projecting certain subsets of lattices from a higher dimensional space $\mathbb{R}^n$ into $\mathbb{R}^d$. This is described by a *cut-and-project scheme*, summarized in the following diagram:

$$\begin{array}{ccccc} E_\parallel \simeq \mathbb{R}^d & \xleftarrow{\pi_\parallel} & E = \mathbb{R}^n & \xrightarrow{\pi_\perp} & E_\perp \simeq \mathbb{R}^m \\ \cup & \nwarrow_{1\text{–}1} & \cup & \nearrow_{\text{dense}} & \cup \\ L_\parallel = \pi_\parallel(L) & & L \text{ lattice} & & W \text{ polytope} \end{array}$$

It consists of a Euclidean vector space E, together with orthogonal projections $\pi_\parallel$ and $\pi_\perp$. The vector spaces $E_\parallel = \pi_\parallel(E)$ and $E_\perp = \pi_\perp(E)$ are called *direct* and *internal* space, respectively. Let $L \subset E$ be a lattice. The projections are such that $\pi_\parallel|_L$ is one to one and $\pi_\perp(L)$ is dense in $E_\perp$ (or dense in some subspace of $E_\perp$). Let $W \subset E^\perp$ be a polytope (or a finite union of polytopes). The set W is also called the *acceptance window*. The set of tiling vertices $\Lambda(W)$ is defined by

$$\Lambda(W) = \{\mathbf{x}_\parallel \in L_\parallel \mid \mathbf{x} \in L \text{ and } \mathbf{x}_\perp \in W\}. \tag{1}$$

The edges of the tiling are defined by the following rule: the tiling vertices $\pi_\parallel(\mathbf{x})$ and $\pi_\parallel(\mathbf{y})$ are adjacent iff the lattice vectors $\mathbf{x}$ and $\mathbf{y}$ are adjacent.

For the Ammann-Beenker tiling [1, 18], we have $n = 4$ and $d = m = 2$. The lattice is $L = \mathbb{Z}^4$. The projections $\pi_\parallel$ and $\pi_\perp$ are defined as follows. For $\mathbf{x} \in \mathbb{R}^n$, we set

$$\begin{aligned} \mathbf{x}_\parallel &= \begin{pmatrix} 1 & \cos\frac{\pi}{4} & \cos\frac{2\pi}{4} & \cos\frac{3\pi}{4} \\ 0 & \sin\frac{\pi}{4} & \sin\frac{2\pi}{4} & \sin\frac{3\pi}{4} \end{pmatrix} \mathbf{x} \\ \mathbf{x}_\perp &= \begin{pmatrix} 1 & \cos\frac{3\pi}{4} & \cos\frac{6\pi}{4} & \cos\frac{9\pi}{4} \\ 0 & \sin\frac{3\pi}{4} & \sin\frac{6\pi}{4} & \sin\frac{9\pi}{4} \end{pmatrix} \mathbf{x}. \end{aligned} \tag{2}$$

The acceptance window $W \subset \mathbb{R}^m$ is a regular octagon with unit side length centred at the origin, having edges perpendicular to the axes. A typical patch is shown in figure 1.

For the rhombic Penrose tiling [6, 27], we have $n = 5, d = 2$ and $m = 3$. The lattice is $L = \mathbb{Z}^5$. The projections $\pi_\parallel$ and $\pi_\perp$ are, for $\mathbf{x} \in \mathbb{R}^n$, defined by

$$\begin{aligned} \mathbf{x}_\parallel &= \begin{pmatrix} 1 & \cos\frac{2\pi}{5} & \cos\frac{4\pi}{5} & \cos\frac{6\pi}{5} & \cos\frac{8\pi}{5} \\ 0 & \sin\frac{2\pi}{5} & \sin\frac{4\pi}{5} & \sin\frac{6\pi}{5} & \sin\frac{8\pi}{5} \end{pmatrix} \mathbf{x} \\ \mathbf{x}_\perp &= \begin{pmatrix} 1 & \cos\frac{4\pi}{5} & \cos\frac{8\pi}{5} & \cos\frac{12\pi}{5} & \cos\frac{16\pi}{5} \\ 0 & \sin\frac{4\pi}{5} & \sin\frac{8\pi}{5} & \sin\frac{12\pi}{5} & \sin\frac{16\pi}{5} \\ 1 & 1 & 1 & 1 & 1 \end{pmatrix} \mathbf{x}. \end{aligned} \tag{3}$$

The acceptance window $W \subset \mathbb{R}^m$ is made up of four regular pentagons in the planes $\mathbf{x}_{\perp 3} = 0, 1, 2, 3$. The pentagons in the 0 and 3 x_3-planes have unit side length and the others

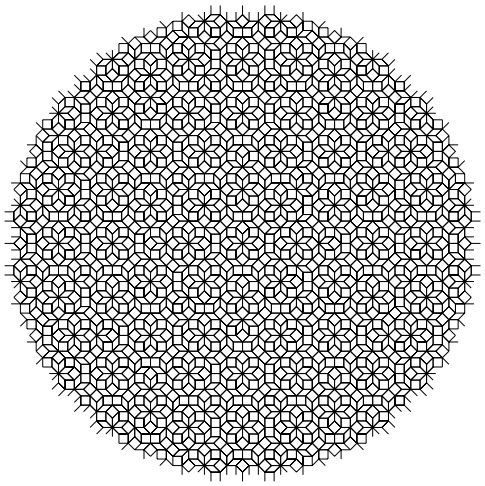

Figure 1. A patch of the Ammann-Beenker tiling.

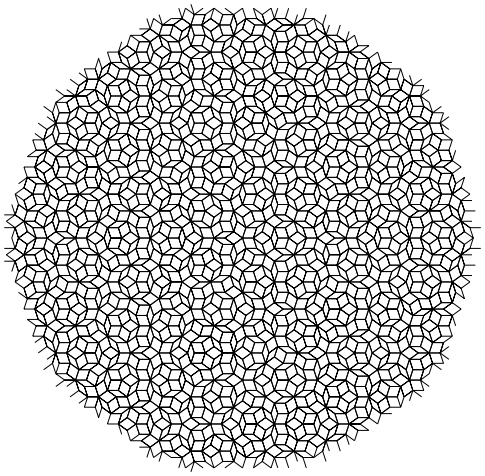

Figure 2. A patch of the rhombic Penrose tiling.

have side length $2\cos\frac{\pi}{5}$. Each pentagon is centred at $\mathbf{x}_{\perp 1} = 0$, $\mathbf{x}_{\perp 2} = 0$. Pentagons 0 and 2 have an edge crossing the positive $\mathbf{x}_{\perp 1}$ axis at right angles while pentagons 1 and 3 are rotated through $\frac{\pi}{5}$. A typical patch is shown in figure 2.

We remark in passing that a more natural embedding of the rhombic Penrose tiling is the root lattice A_4, see also [3], but $\mathbb{Z}^5$ is more convenient for computations. Moreover, the Ammann-Beenker tiling and the rhombic Penrose tiling may be alternatively defined by inflation rules for their prototiles [4, 11].

3. Enumeration

A self-avoiding walk on a graph is a path, beginning at an origin vertex, which never visits a vertex more than once. The SAW on the lattice $\mathbb{Z}^d$ is a well-studied object (see, for example, [23, 26]). The number c_n of translationally inequivalent n-step walks on a regular lattice is

Table 1. The number of n-step fixed origin SAWs for various starting points $\mathbf{x}_\perp$ in the Ammann-Beenker tiling, with starting point coordinates (x, y) given in the internal space.

n	$\mathbf{x}_\perp = (0, 0)$	$\mathbf{x}_\perp = (1, 0)$	$\mathbf{x}_\perp = (1 - \frac{\sqrt{2}}{2}, \frac{\sqrt{2}}{2})$	$\mathbf{x}_\perp = (1 - \sqrt{2}, 0)$
0	1	1	1	1
1	8	3	4	5
2	16	13	12	16
3	48	34	46	42
4	144	108	108	152
5	448	292	374	388
6	1 088	952	976	1 194
7	3 680	2 458	3 042	3 412
8	9 584	7 746	8 330	9 678
9	28 336	21 348	24 556	27 218
10	82 960	61 478	68 376	79 150
11	225 408	177 230	197 820	217 562
12	657 536	495 808	554 108	628 996
13	1 834 768	1 412 152	1 576 464	1 741 464
14	5 140 752	3 985 706	4 400 920	4 968 606
15	14 584 112	11 125 408	12 531 794	13 724 682
16	40 222 672	31 617 786	34 541 864	39 209 054
17	114 683 280	87 149 372	98 846 548	107 503 768
18	313 146 848	248 799 302	270 221 012	306 845 714
19	896 810 944	680 172 768	773 046 904	840 463 852
20	2 437 468 000	1 943 692 238	2 109 562 128	2 386 875 508
21	6 958 267 152	5 303 535 884	6 011 045 200	6 548 653 714
22	18 981 078 176	15 086 983 820	16 431 248 782	18 500 898 140
23	53 728 620 912	41 295 324 398	46 538 635 588	50 883 461 478
24	147 472 084 608	116 624 466 842	127 704 810 544	142 927 122 532
25	413 887 940 176			

clearly independent of the choice of origin vertex. Hence this series is representative of the entire lattice. The enumeration of SAWs on non-periodic tilings introduces complications to the interpretation of the series $C(x) = \sum_{n \geqslant 0} c_n x^n$. This is because the possible origin vertices produce an infinite range of different series $C(x)$. Each origin produces a different series which is representative only of that vertex's immediate neighbourhood in the tiling. The question then is: how do we obtain a SAW series which is representative of the whole tiling? In this paper we adopt three different approaches to enumerating SAWs on quasiperiodic tilings, as described in the introduction. They are

- *fixed origin walks,*
- *mean number of walks,*
- *total number of walks.*

3.1. Fixed origin walks

We take a random selection of origin vertices $\mathbf{x} \in L$ (if $\mathbf{x}_\perp \notin W$ the vertex is not a suitable choice and is ignored). For each suitable origin, we generate the neighbourhood of the vertex, including all vertices up to some Euclidean distance N away. Two such neighbourhoods are shown in figures 1 and 2. We enumerate all SAWs from the origin up to length n in the neighbourhood using backtracking [31]. This takes time proportional to the number of walks c_n. Unfortunately, the transfer matrix approaches used to enumerate SAWs on

Table 2. The number of fixed origin n-step SAWs for various starting points $\mathbf{x}_\perp$ in the rhombic Penrose tiling, with starting point coordinates (x, y, z) given in the internal space.

n	$\mathbf{x}_\perp = (0, 0, 1)$	$\mathbf{x}_\perp = (0, 0, 0)$	$\mathbf{x}_\perp = (0.5, 0.5, 1)$	$\mathbf{x}_\perp = (0.25, 0.5, 0)$
0	1	1	1	1
1	5	5	5	4
2	20	10	14	12
3	40	40	50	46
4	160	130	130	112
5	450	310	406	394
6	1 170	1 140	1 177	938
7	4 000	2 680	3 316	3 416
8	9 480	9 360	9 723	7 866
9	32 910	23 150	27 356	27 312
10	76 090	72 520	77 747	66 150
11	262 250	196 980	224 102	215 924
12	619 460	555 290	615 549	545 062
13	2 050 500	1 646 990	1 812 802	1 698 548
14	5 052 310	4 292 010	4 869 786	4 411 293
15	15 828 550	13 403 280	14 455 725	13 367 278
16	41 103 090	33 637 420	38 524 509	35 243 859
17	121 759 470	106 779 600	114 089 288	105 117 832
18	331 072 990	265 198 150	304 434 061	279 216 083
19	937 563 530	840 669 610	894 584 372	825 140 032
20	2 642 381 430	2 092 703 550	2 399 386 239	2 199 738 033
21	7 227 151 280	6 573 888 100	6 988 332 717	6 459 329 037
22	20 931 973 090	16 491 425 740	18 844 561 759	17 267 339 059
23	55 793 302 330	51 185 968 460	54 473 434 666	50 419 312 152
24	164 764 171 030	129 673 789 110	147 471 723 662	135 162 732 506

regular two-dimensional lattices in less time cannot be used in this problem without major adaptation: since a SAW of N steps may reach a vertex N steps from the origin, we would need to consider every possible tiling patch of radius N. The finite-lattice method's transfer matrix stage would then need to be adapted to each tiling patch, or generalized to handle them all.

If we apply this method to counting walks on a regular lattice it is clear that we would always produce the usual SAW series for that lattice. If each of the series in tables 1 and 2 showed lattice consistent properties, it would be a good indication that these properties belong to the entire tiling. The actual neighbourhoods chosen for the enumerations are shown in figures 3 and 4 for the Ammann-Beenker and Penrose tilings, respectively.

3.2. Mean number of walks

Given that a pair of vertices from $\Lambda(W)$ are adjacent if and only if they are adjacent in L, we see that the neighbours of a vertex with image $\mathbf{x}_\perp$ can be found by sequentially adding the $E_\perp$ image of all possible edges in L to $\mathbf{x}_\perp$ and testing if the new points lie in W. If it does the adjacent vertex exists in $\Lambda(W)$. By recursively checking all possible neighbours of a vertex, all possible walks on the lattices will be found.

Given an origin vertex x^0 in $\Lambda(W)$, we know its $E_\perp$ image $x_\perp^0$ must lie somewhere in W, i.e. $x_\perp^0 \in W^0 = W$ (W^n is the region $x_\perp^0$ can lie in given our knowledge of the n steps in the walk). If we take a step s (with projection $s_\perp$ onto $E_\perp$) to a possible adjacent vertex

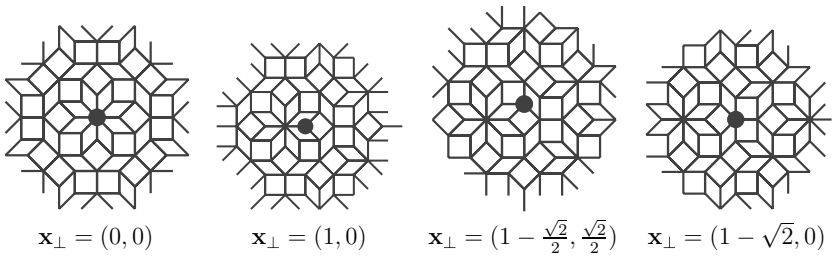

Figure 3. The actual Ammann-Beenker neighbourhoods chosen for the enumerations.

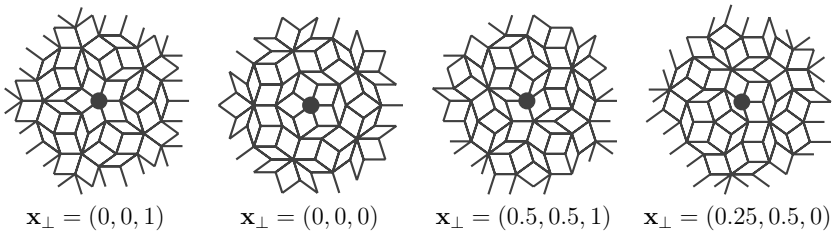

Figure 4. The actual rhombic Penrose neighbourhoods chosen for the enumerations.

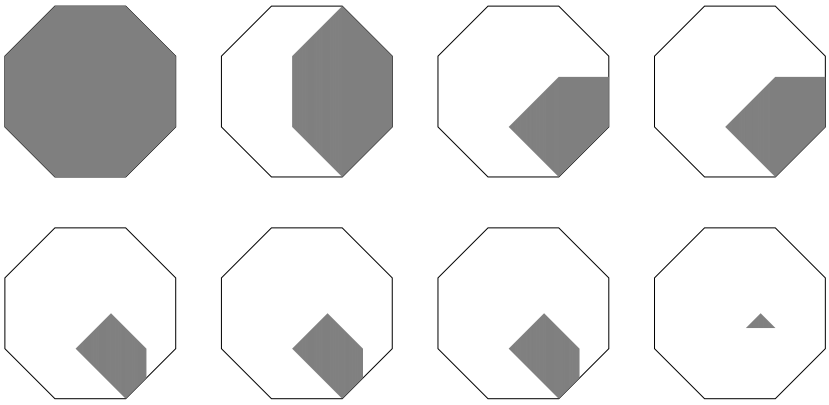

Figure 5. Examples of $W^0 \ldots W^7$ for a particular walk on the Ammann-Beenker tiling.

x^1, then we know $x^1_\perp = x^0_\perp + s_\perp$. Furthermore, if $x^1 \in \Lambda(W)$ is true, $x^1_\perp \in W$. Hence $W^1 = (W \cap (W^0 + s_\perp)) - s_\perp$. The probability that the step s is possible from a random x^0 is given by the ratio between the areas of W^1 and W.

Extending this to a walk of length n with steps s^i, $i = 1, \ldots, n$, $W^k = \left(W \cap \left(W^{k-1} + \sum_{i=1}^{k} s^i_\perp\right)\right) - \sum_{i=1}^{k} s^i_\perp$, the probability of the walk existing is the ratio of the areas of W^n and W. For example, consider the shaded W^i in figure 5, for the particular walk in the Ammann-Beenker tiling which steps west, south, south-west, north-west, west, north then north. For the Ammann-Beenker tiling, these probabilities are of the form $a + b\lambda$, where $\lambda = 1 + \sqrt{2}$ and $a, b \in \mathbb{Q}$.

Adding the self-avoiding constraint and summing the probabilities results in the expected number of SAWs beginning at a random origin. Again note that applying this method to a regular lattice would result in the usual SAW series. Due to the extra complexity of the

Table 3. The mean number of n-step SAWs for the Ammann-Beenker tiling and the rhombic Penrose tiling, where $\lambda = 1 + \sqrt{2}$ and $\tau = (1 + \sqrt{5})/2$.

n	Ammann-Beenker	Rhombic Penrose
0	1	1
1	4	4
2	$52 - 16\lambda$	$62 - 30\tau$
3	$80 - 16\lambda$	$-4 + 28\tau$
4	$444 - 134\lambda$	$914 - 488\tau$
5	$1280 - 380\lambda$	$-820 + 732\tau$
6	$4492 - 1430\lambda$	$13842 - 7894\tau$
7	$10848 - 3248\lambda$	$-17732 + 12860\tau$
8	$60988 - 21700\lambda$	$173876 - 101988\tau$
9	$89800 - 27036\lambda$	$-255784 + 173720\tau$
10	$643248 - 237732\lambda$	$1923078 - 1143988\tau$
11	$979776 - 324200\lambda$	$-3149856 + 2073192\tau$
12	$5486960 - 2043420\lambda$	$19566548 - 11734706\tau$
13	$10785736 - 3819788\lambda$	$-34951044 + 22612992\tau$
14	$45253532 - 16927618\lambda$	$192557132 - 116151274\tau$
15	$110294592 - 40576780\lambda$	$-366912524 + 234803904\tau$
16	$375796808 - 141368464\lambda$	
17	$1058437232 - 398339560\lambda$	
18	$3259350860 - 1238175678\lambda$	
19	$9526156024 - 3632872284\lambda$	
20	$29127575440 - 11192322668\lambda$	
21	$81536068712 - 31337365980\lambda$	
22	$259724099656 - 100797073134\lambda$	

rhombic Penrose tiling acceptance window, the area calculations are more involved, see also [28]. They lead to mean numbers of the form $a + b\tau$, where $\tau = (1 + \sqrt{5})/2$ is the golden number, and $a, b \in \mathbb{Z}$. The rhombic Penrose tiling also allows steps in ten directions, more than the Ammann-Beenker tiling's eight. These facts combine to allow greater length series to be computed on the Ammann-Beenker tiling. The corresponding mean numbers of SAWs are given in table 3.

3.3. Total number of walks

Investigating all possible walks as in the mean number of walks method, we count instead the number of non-zero contributions to the mean value. This counts the number of translationally inequivalent walks with W^n having positive area or, equivalently, the number of translationally inequivalent walks which may occur anywhere in the tiling. Again we note that applying this method to a regular lattice gives the usual SAW series. The numbers are given in table 4.

3.4. Self-avoiding polygons

A self-avoiding polygon is equivalent to a self-avoiding walk in which the initial and final vertices are adjacent. In the enumeration of self-avoiding polygons, we do not distinguish between polygons having, up to a translation, the same boundary but different fillings of the interior.

SAPs may be enumerated in the same manner as we enumerate SAWs. The additional property of end point adjacency allows the backtracking algorithm to be pruned earlier. When enumerating SAPs up to size N, a walk that visits a vertex after D steps that is further than

Table 4. The total number of n-step SAWs for the Ammann-Beenker tiling and the rhombic Penrose tiling.

n	Ammann-Beenker	Penrose
0	1	1
1	8	10
2	56	90
3	288	560
4	1 280	2 800
5	5 344	12 060
6	20 288	48 520
7	74 192	182 000
8	260 336	658 300
9	892 800	2 282 400
10	2 976 512	7 749 440
11	9 828 256	25 634 920
12	31 758 112	83 615 140
13	101 847 216	268 113 660
14	322 240 144	850 895 040
15	1 012 048 208	2 668 534 600
16	3 147 031 584	
17	9 732 815 728	
18	29 852 932 384	
19	91 182 029 360	
20	276 695 822 928	
21	836 719 766 336	
22	2 516 664 888 416	

$N - D$ steps from the origin may be pruned from the search tree. Such a walk can never form part of a SAP of $\leqslant N$ steps. This was used to extend the length of the rhombic Penrose SAP series. The Ammann-Beenker SAP series were calculated at the same time as the SAW series and hence are of the same length. The extensive run time requirements precluded further series extension.

For the computation of occurrence probabilities of self-avoiding polygons, the loop vertices are taken into account, as described in section 3.2 for the mean number of walks. If the self-avoiding polygon has n loop vertices $x^i \in \Lambda(W)$, where $i = 1, \ldots, n$, the acceptance domain is $W^n = \bigcap_i \left(W - x^i_\perp\right)$, and the occurrence probability is given by the ratio between the areas of W^n and W, see also [28]. The corresponding numbers are shown in table 5.

4. Analysis of series

The various sequences were analysed using standard methods of asymptotic analysis of power series expansions as described in [12]. For self-avoiding walks and polygons on the square lattice, it is easy to prove that the limit $\lim_{n\to\infty}(c_n)^{1/n}$ exists by use of concatenation arguments [26]. We assume the usual asymptotic growth of the sequence coefficients c_n, namely

$$c_n = A x_c^{-n} n^{\gamma-1}[1 + \mathcal{O}(n^{-\varepsilon})] \qquad (n \to \infty, 0 < \epsilon \leqslant 1). \tag{4}$$

On the square lattice, there is overwhelming evidence [8] of the above asymptotic behaviour with $\gamma = 43/32$. There is however no proof of this assumption. For interesting new

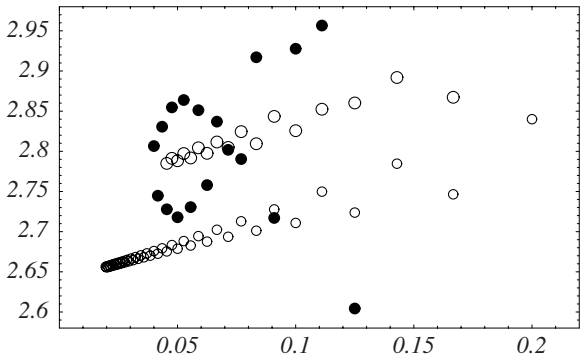

Figure 6. Ratio plot of c_n/c_{n-1} against $1/n$ for fixed origin (full circles) and mean number (large open circles) Ammann-Beenker SAWs. The square lattice SAW data are plotted with small circles for comparison.

Table 5. The mean number of n-step SAPs and the total number of SAPs for the Ammann-Beenker tiling (first two columns) and for the rhombic Penrose tiling (last two columns), where $\lambda = 1+\sqrt{2}$ and $\tau = (1+\sqrt{5})/2$.

n	Mean number	Total number	Mean number	Total number
2	4	8	4	10
4	8	48	8	80
6	12λ	384	$108-48\tau$	840
8	$800-272\lambda$	2 960	$240-64\tau$	6 480
10	$2840-880\lambda$	21 600	$6192-3364\tau$	49 760
12	$28152-9984\lambda$	170 256	$25584-13248\tau$	394 080
14	$47712-9884\lambda$	1 322 048	$179200-95340\tau$	3 087 140
16	$869600-299392\lambda$	10 194 720	$162976-5440\tau$	24 020 160
18	$215712+294408\lambda$	79 960 896	$2704140-1067580\tau$	183 529 440
20	$14980920-3730840\lambda$	618 248 240		
22	$152588920-47048100\lambda$	4 726 263 168		

developments see [23]. The above assumption results in an asymptotic growth of the ratios r_n

$$r_n = \frac{c_n}{c_{n-1}} = \frac{1}{x_c}\left[1+\frac{\gamma-1}{n}+\mathcal{O}(n^{-1-\varepsilon})\right] \qquad (n\to\infty, 0<\epsilon\leqslant 1) \qquad (5)$$

which may be used to extrapolate numerical estimates of x_c and γ. Whereas it has been proved for the square lattice that the limit $\lim_{n\to\infty} c_n/c_{n-2}$ exists and coincides with x_c^{-2} [19], a similar statement for the ratios r_n is not known. For some lattices, counterexamples are known [13].

Figure 6 shows a plot of the ratios r_n against $1/n$ for a typical fixed origin Ammann-Beenker walk (full circles) and for the ratios of the mean numbers of Ammann-Beenker walks (large open circles). We notice that the fixed origin data suffer from dramatic fluctuations, which are smoothed out by averaging, but are still larger than the corresponding square lattice data [8], which are shown by small circles. The oscillating behaviour of the mean number of walks data is due to an additional singularity of the sequence generating function at $x=-x_c$, which, for the case of the square lattice, is well understood due to anti-ferromagnetic ordering [8]. To obtain estimates of x_c and γ, we used the standard method described in [12] and first mapped away the singularity on the negative real axis by a Euler transform and then used Neville–Aitken series extrapolation.

Table 6. Estimates of x_c and γ for Ammann-Beenker SAWs. Numbers in parentheses denote the uncertainty in the last two digits.

	Mean no	$(0, 0)$	$(1-\frac{\sqrt{2}}{2}, \frac{\sqrt{2}}{2})$	$(1, 0)$	$(1-\sqrt{2}, 0)$
x_c	0.36414(18)	0.3659(14)	0.3644(13)	0.3644(21)	0.3657(16)
γ	1.325(19)	1.45(16)	1.30(14)	1.32(17)	1.46(17)

We also used the method of differential approximants (DAs) [12]. The underlying idea is to fit a linear differential equation with polynomial coefficients to the generating function of the sequence, truncated at some order n_0. The critical points and critical exponents of the differential equation are expected to approximate the critical behaviour of the underlying sequence. Application of first-order and second-order DAs has proved useful for the analysis of square lattice SAWs [12]. A first-order DA involves fitting the coefficients to the differential equation $P_1(x)xf'(x) + P_0(x)f(x) = R(x)$ where $P_1(x)$, $P_0(x)$ and $R(x)$ are polynomials of degree N, M and L, respectively. We refer to this as a $[L/M; N]$ DA. We analysed the approximants $[L/N-1; N]$, $[L/N; N]$, $[L/N+1; N]$ for $1 \leqslant L \leqslant 8$. We computed estimates for x_c and γ by averaging the different DA results, given a fixed number of series coefficients n_0. Since this yields more accurate estimates of x_c and γ (typically of one digit better) than the ratio method and series extrapolation, we list in table 6 only the results for the DA analysis. Note that the errors are no strict error bounds, but arise from averaging over approximants $[L/N_0; N_1]$ for different values of N_0, N_1 and L, as explained in [12].

As suggested by the ratio plot, the estimate using the data for the mean number of walks yields the most precise estimates, which are, however, one order of magnitude in error worse than the corresponding estimates for square lattice SAWs.

An analysis of the total number of SAWs on the Ammann-Beenker tiling using first-order DAs yields $x_c = 0.3647(33)$ and $\gamma = 3.14(37)$. Whereas the critical point estimate is consistent with the previous analysis, the exponent estimate deviates from the value of $43/32 = 1.343\,75$ for fixed origin SAWs or the mean number of SAWs. This phenomenon reflects the fact that the number of Ammann-Beenker patches of radius r increases asymptotically as r^2. (More generally, for aperiodic Delone sets in $\mathbb{R}^d$ described by a primitive substitution matrix, the number $N(r)$ of patches of radius r increases like $N(r) \simeq r^d$ [21, 24].) Since the SAW has fractal dimension $4/3$, we expect an asymptotic increase of the number of SAWs by $n^{2\nu}$, where $\nu = 3/4$. Thus $\gamma = 43/32 + 2\nu = 2.843\,75$. Data extrapolation is consistent with this value.

The analysis of SAP data follows the same lines. However, the estimates suffer from large finite-size errors due to the less number (11) of available coefficients. First-order differential approximants for the mean number of SAPs yield $x_c = 0.3688(41)$. We assume $x_c(SAP) = x_c(SAW)$, which has been proved for the square lattice case [14].

For the critical exponent $\alpha = 2 + \gamma$, we expect for the mean number of SAPs by universality that $\alpha = 1/2$, being the believed exact value for the square lattice (and numerically confirmed to very high precision [16]). Due to lack of data it is not possible to give estimates of critical exponents. An analysis of the total number of SAPs on the Ammann-Beenker tiling using first-order DAs yields $x_c = 0.3587(15)$.

The above analysis has also been applied to the rhombic Penrose tiling data. We observe qualitatively the same finite size behaviour as for the Ammann-Beenker tiling data, though the fluctuations are a bit less pronounced. In table 7 we list estimates for x_c and γ obtained by analysing first-order differential approximants.

An analysis of the total number of SAWs on the rhombic Penrose tiling using first-order DAs yields $x_c = 0.3638(31)$ and $\gamma = 2.77(21)$. The estimate of the critical point is consistent

Table 7. Estimates of x_c and γ for Penrose SAWs. Numbers in parentheses denote the uncertainty in the last two digits.

	Mean no	(0, 0, 0)	(0, 0, 1)	(0.25, 0.5, 0)	(0.5, 0.5, 1)
x_c	0.36322(29)	0.3621(12)	0.3613(16)	0.36248(83)	0.36347(51)
γ	1.333(26)	1.28(14)	1.19(22)	1.303(83)	1.387(62)

with the estimates from the other methods of counting. For the critical exponent, we again expect a value of $\gamma = 43/32 + 2\nu = 2.843\,75$, which agrees with the extrapolation within numerical accuracy.

For the analysis of SAP data, only nine series coefficients are available. First-order differential approximants for the mean number of SAPs yield $x_c = 0.372(11)$. An analysis of the total number of SAPs on the rhombic Penrose tiling using first-order DAs yields $x_c = 0.3590(22)$. Again, due to lack of data, it is not possible to extrapolate reasonable estimates for the critical exponent α.

5. Conclusion

We extended previous enumerations for self-avoiding walks and polygons on the Ammann-Beenker tiling and on the rhombic Penrose tiling and extracted estimates for the critical point and critical exponent, using different counting schemes. It turned out that averaging with respect to the occurrence probability in the whole tiling leads to the best estimates, whereas data produced by fixing an origin lead to strong finite-size oscillations. The results support the universality hypothesis that the critical exponents appear to be the same as for the square lattice, within confidence limits. For the total number of walks (polygons) we obtain a new exponent reflecting the polynomial complexity of the number of patches of the underlying tiling.

Since the results were obtained using the enumeration method of backtracking, one might ask if more efficient enumeration methods can be applied in order to substantially increase the length of the series, and hence the accuracy of the estimates. Unfortunately, the successful finite-lattice method cannot be applied in this case, without substantial development.

On a mathematically rigorous level, it may be possible to show the equality of the critical points for SAPs and SAWs on quasiperiodic tilings by appropriately modifying the existing proofs for the hypercubic lattice [14]. Furthermore, it would be interesting to carry out an analysis to determine if random walk behaviour can be proved for dimensions greater than 4 [26].

Self-avoiding polygons may also be counted by area. Since this leads to a three-variable generating function due to the different areas of the prototiles, it is tempting to ask whether the scaling behaviour of these objects is different from that recently found [30] for self-avoiding polygons on two-dimensional lattices.

Acknowledgments

The authors thank Michael Baake for bringing their attention to the above problem and Daniel Lenz for useful advice on substitution systems. CR would like to acknowledge funding by the German Research Council (DFG). AJG would like to acknowledge funding by the Australian Research Council (ARC).

References

[1] Ammann R, Grünbaum B and Shephard G C 1992 Aperiodic tiles *Disc. Comp. Geom.* **8** 1–25

[2] Baake M, Grimm U, Joseph D and Repetowicz P 2000 Averaged shelling for quasicrystals *Mat. Sci. Eng.* A **294–296** 441–5

[3] Baake M, Joseph D, Kramer P and Schlottmann M 1990 Root lattices and quasicrystals *J. Phys. A: Math. Gen.* **23** L1037–41

[4] Baake M and Joseph D 1990 Ideal and defective vertex configurations in the planar octagonal quasilattice *Phys. Rev.* B **42** 8091

[5] Briggs K 1993 Self-avoiding walks on quasilattices *Int. J. Mod. Phys.* B **7** 1569–75

[6] de Bruijn N G 1981 Algebraic theory of Penrose's non-periodic tilings of the plane *Indagationes Mathematicae (Proc. Kon. Ned. Akad. Wet. Ser. A)* **84** 39–52 and 53–66

[7] Conway A R, Enting I G and Guttmann A J 1993 Algebraic techniques for enumerating self-avoiding walks on the square lattice *J. Phys. A: Math. Gen.* **26** 1519–34

[8] Conway A R and Guttmann A J 1996 Square lattice self-avoiding walks and corrections to scaling *Phys. Rev. Lett.* **77** 5284–7

[9] Enting I G 1996 Series expansions from the finite lattice method *Nucl. Phys.* B *(Proc. Suppl)* **47** 180–7

[10] Gähler F, Kramer P, Trebin H-R and Urban K 2000 *Proc. 7th Int. Conference on Quasicrystals, Mat. Sci. Eng.* A **294–296**

[11] Grünbaum B and Shephard G C 1987 *Tilings and Patterns* (New York: Freeman)

[12] Guttmann A J 1989 Asymptotic analysis of power-series expansions *Phase Transitions and Critical Phenomena* vol 13 ed C Domb and J L Lebowitz (London: Academic)

[13] Hammersley J M 1960 Limiting properties of numbers of self-avoiding walks *Phys. Rev.* **118** 656

[14] Hammersley J M 1961 The number of polygons on a lattice *Math. Proc. Cambridge Phil. Soc.* **57** 516–23

[15] Henley C L 1999 Random tiling models *Quasicrystals: The State of the Art* (*Series on Directions in Condensed Matter Physics vol 16*) 2nd edn ed D P DiVincenzo and P J Steinhardt (Singapore: World Scientific) pp 459–560

[16] Jensen I 2000 Size and area of square lattice polygons *J. Phys. A: Math. Gen.* **33** 3533–43

[17] Jensen I and Guttmann A J 1998 Self-avoiding walks, neighbour-avoiding walks and trails on semiregular lattices *J. Phys. A: Math. Gen.* **31** 8137–45

[18] Katz A 1995 Matching rules and quasiperiodicity: the octagonal tiling *Beyond Quasicrystals* ed F Axel and D Gratias (Berlin: Springer) pp 141–89

[19] Kesten H 1963 On the number of self-avoiding walks *J. Math. Phys.* **4** 960–9

[20] Kramer P and Neri R 1984 On periodic and non-periodic space-fillings of E^m obtained by projection *Acta Cryst.* A **40** 580–7

Kramer P and Neri R 1984 On periodic and non-periodic space-fillings of E^m obtained by projection *Acta Cryst.* A **41** 619 (erratum)

[21] Lagarias J C and Pleasants P A B 2001 Local complexity of Delone sets and crystallinity *Preprint* math.MG/0105088

[22] Langie G and Iglói F 1992 Walks on the Penrose lattice *J. Phys. A: Math. Gen.* **25** L487–91

[23] Lawler G F, Schramm O and Werner W 2002 On the scaling limit of planar self-avoiding walk *Preprint* math.PR/0204277

[24] Lenz D 2002 Private communication

[25] Luck J M 1993 A classification of critical phenomena on quasi-crystals and other aperiodic structures *Europhys. Lett.* **24** 359–64

[26] Madras N and Slade G 1993 *The Self-Avoiding Walk* (Boston, MA: Birkhauser)

[27] Penrose R 1974 The rôle of aesthetics in pure and applied mathematical research *Bull. Inst. Math. Appl. (Southend-on-Sea)* **10** 266–71

[28] Repetowicz P, Grimm U and Schreiber M 1999 High-temperature expansion for Ising models on quasiperiodic tilings *J. Phys. A: Math. Gen.* **32** 4397–418

[29] Repetowicz P 2002 Finite-lattice expansion for the Ising model on the Penrose tiling *J. Phys. A: Math. Gen.* **35** 7753–72

[30] Richard C, Guttmann A J and Jensen I 2001 Scaling function and universal amplitude combinations for self-avoiding polygons *J. Phys. A: Math. Gen.* **34** L495–501

[31] Sedgewick R 1992 *Algorithms in C++* 2nd edn (Reading, MA: Addison-Wesley)